# Atmospheric effects on extensive air showers observed with the array of surface detectors of the Pierre Auger Observatory

**Benjamin Rouillé d'Orfeuil*** **for the Pierre Auger Collaboration**†

*Laboratoire AstroParticule et Cosmologie, Université Paris 7, CNRS-IN2P3
†Observatorio Pierre Auger, Av. San Martin Norte 304, (5613) Malargüe, Mendoza, Argentina

***Abstract*. Atmospheric parameters, such as pressure (P), temperature (T) and density ($\rho \propto$ P/T), affect the development of extensive air showers (EAS) initiated by energetic cosmic rays. We have studied the impact of atmospheric variations on EAS with data from the array of surface detectors of the Pierre Auger Observatory, analysing the dependence of the event rate on P and $\rho$. We show that the observed behaviour is explained by a model including P and $\rho$ and validated with full EAS simulations. Changes in the atmosphere affect also the measured signal, with an impact on the determination of the energy of the primary particle. We show how the energy estimation can be corrected for such effects.**

***Keywords*: EAS, UHECR, atmosphere**

## I. Introduction

High-energy cosmic rays (CRs) are detected by means of the extensive air shower (EAS) they produce in the atmosphere. The atmosphere affects the EAS development. The properties of the primary CR, such as its energy, have to be inferred from EAS. Therefore the study and understanding of the effects of atmospheric variations on EAS in general, and on a specific detector in particular, is very important for the comprehension of the detector performances and for the correct interpretation of EAS measurements.

We have studied the impact of atmospheric variations on EAS with data collected during 4 years with the array of surface detectors (SD) of the Pierre Auger Observatory, located in Malargüe, Argentina. The Pierre Auger Observatory is designed to study CRs from $\approx 10^{18}$ eV up to the highest energies. The SD consists of 1600 water-Cherenkov detectors to detect the photons and the charged particle of the EAS. It is laid out over 3000 km$^2$ on a triangular grid of 1.5 km spacing and is overlooked by 24 fluorescence telescopes (FD) grouped in units of 6 at four locations on its periphery. For each event, the signals in the stations are fitted to find the signal at a 1000 m core distance, S(1000), which is used to estimate the primary energy.

## II. Impact of atmospheric effects on EAS and their measurement

The water-Cherenkov detectors are sensitive to both the electromagnetic (e.m) component and the muonic component of the EAS, which are influenced to a different extent by atmospheric variations. These in turn influence the signal measured in the detectors and in particular S(1000) [1]. Pressure (P) and air density ($\rho$) are the properties of the atmosphere that affect EAS the most. P changes are associated to changes in the column density of the air above the detector, and hence affect the age of the EAS when they reach the ground. $\rho$ changes modify the Molière radius ($r_M$) and thus influence the lateral attenuation of the EAS. The impact on S(1000) can then be modeled with a Gaisser-Hillas and Nishimura-Kamata-Greisen profile, which describe respectively the longitudinal and the lateral distribution of the e.m component of the EAS. In fact, the relevant value of $r_M$ is the one corresponding to the air density two radiation lengths ($X_0$) above ground in the direction of the incoming EAS [2]. Due to the thermal coupling of the lower atmosphere with the Earth surface, the variation of $\rho$ at $2X_0$ is the same as at the ground on large time scales, while it is smaller on shorter time intervals. It is then useful to separate the dependence of the total signal $S = S_{em} + S_\mu$ on $\rho$ in two terms describing respectively its longer term modulation and its daily one. Introducing the average daily density $\rho_d$ and the instantaneous departure from it, $\rho - \rho_d$, we have:

$$S = S_0\,[1+\alpha_P(P-P_0)+\alpha_\rho(\rho_d-\rho_0)+\beta_\rho(\rho-\rho_d)] \quad (1)$$

where $S_0$ is the signal that would have been measured at some reference atmospheric conditions with pressure $P_0$ and density $\rho_0$.

The fraction of the signal at 1 km of the core due to the e.m particles is taken as $F_{em} = F_0 - 0.5(\sec\theta - 1)$ with $F_0 = 0.65 + 0.035\log(E/\mathrm{EeV})$ that provides a reasonable fit to the results of proton EAS simulated for zenith angle $\theta < 60°$ and energies $E = 10^{18}$ to $10^{19}$ eV. The P correlation coefficient is:

$$\alpha_P \simeq -\frac{F_{em}}{g}\left[1 - \frac{\hat{X}_m}{X}\right]\frac{\sec\theta}{\Lambda}$$

where $X = X_v \sec\theta$ is the slant depth with $X_v = 880$ g cm$^{-2}$ the grammage at the detector site. $\Lambda$ is an effective attenuation length associated to the longitudinal development of the EAS at 1 km from their core and $g$ is the acceleration of gravity. The depth of the EAS maximum at 1 km from the core is $\hat{X}_m \simeq X_m + 150$ g cm$^{-2}$, with $X_m \simeq [700 + 55\log(E/\mathrm{EeV})]$ g cm$^{-2}$ being the average value of the EAS maximum at the core measured by the FD [4]. Due to the flat longitudinal development of the muons, no significant P dependence is expected

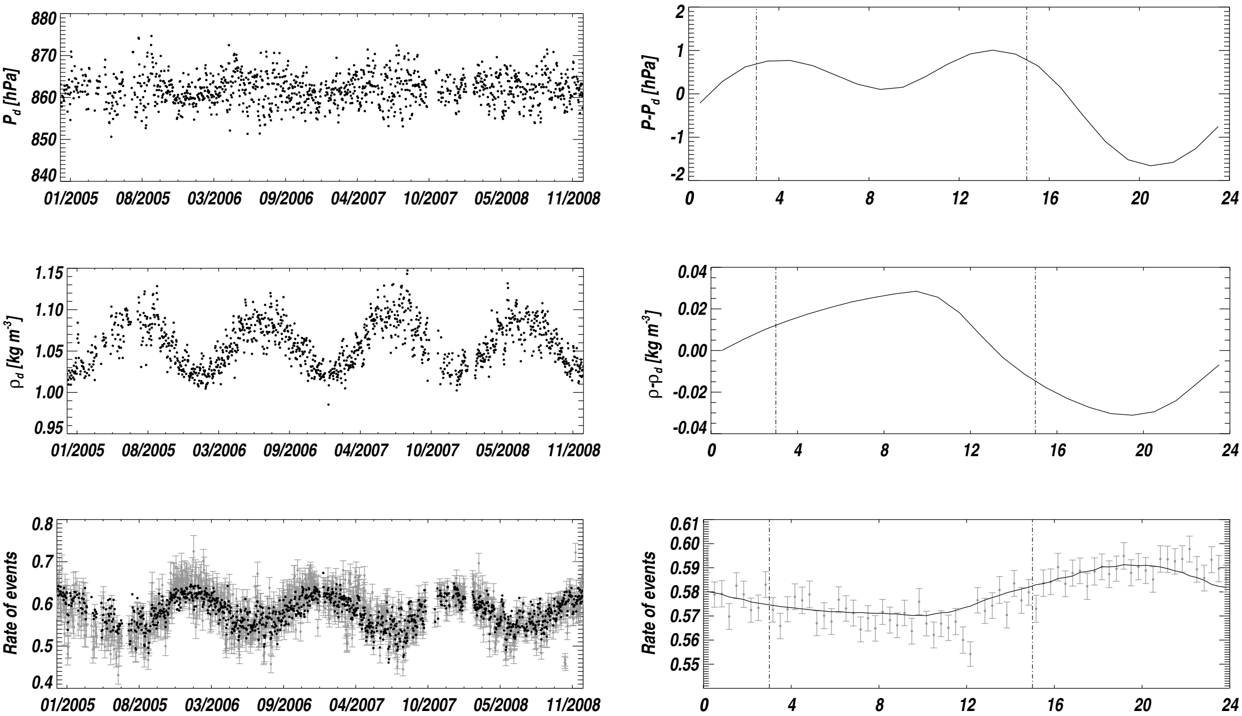


Fig. 1. Left: daily averages of ground P (top), $\rho$ (middle) and rate of events (bottom, grey). The prominent effect on the modulation of the rate of events is due to $\rho$ variations. The black points in the bottom plot show the results of the fit. Right: variation of P (top), $\rho$ (middle) and the rate of events during the day (UTC). The vertical dashed lines show the local midnight and noon (UTC-3h) and the black line in the bottom plot show the result of the fit.

for the muonic component. The $\rho$ correlation coefficient describing the daily averaged modulation of S is:

$$\alpha_\rho \simeq F_{em}\,\alpha_\rho^{em} + (1 - F_{em})\,\alpha_\rho^{\mu}$$

with:

$$\alpha_\rho^{em} = -\frac{4.5 - 2s}{\rho_0}$$

where $s = 3/(1 + 2\cos\theta X_m/X_v)$ is the shower age. $\alpha_\rho^{\mu}$ is found to be consistent with a zero value in the proton EAS simulations. Concerning the modulation on short time scale, we adopt $\beta_\rho = F_{em}\,\beta_\rho^{em}$ with:

$$\beta_\rho^{em} = \exp(-a\cos\theta)\,\alpha_\rho^{em}$$

where $a$ characterises the amplitude of the daily $\rho$ variation in the lower atmosphere and is completely independent of the EAS development.

As atmospheric variations correspond to signal variations, this implies that the same primary CR will induce different signals depending on P and $\rho$. It follows that the rate of events observed in a given range of S(1000) will be modulated in time. The effect can be quantified starting from the relation between S(1000) and the reconstructed energy: $E_r \propto [S(1000)]^B$, where $B = 1.08{\pm}0.01(\mathrm{stat}){\pm}0.04(\mathrm{sys})$ [3]. Following eq. (1), the primary energy $E_0(\theta, P, \rho)$ that would have been obtained for the same EAS at the reference atmospheric conditions is related to $E_r$ as follows:

$$E_0 = E_r\,[1 - \alpha_\xi\Delta\xi]^B \qquad (2)$$

where $\alpha_\xi\Delta\xi \equiv \alpha_P(P - P_0) + \alpha_\rho(\rho_d - \rho_0) + \beta_\rho(\rho - \rho_d)$. If we focus on a given $\theta$ bin, the rate of events per unit time in a given signal range, $[S_m, S_M]$ is:

$$R(S_m, S_M) = \int_{S_m}^{S_M} \mathrm{d}S\,A(S)\,\frac{\mathrm{d}J}{\mathrm{d}S}$$

where J is the flux of CRs and $A(S)$ is the instantaneous acceptance of the experiment. It will be of the form $A(S) = \kappa\,\epsilon(S)$, where $\kappa$ is a constant global factor proportional to the area of the SD and the solid angle considered, while $\epsilon(S)$ is the trigger probability. Assuming that the CR spectrum is a pure power law, *i.e* $\mathrm{dJ/dE_0} \propto \mathrm{E_0^{-\gamma}}$, and using eq. (2) and neglecting the small energy dependence of the coefficients $\alpha_\xi$, we can derive the corresponding dependence of the rate of events:

$$R(S_m, S_M) \propto (1 + a_\xi\Delta\xi)\int_{S_m}^{S_M} \mathrm{d}S\,\epsilon(S)\,S^{-B\gamma+B-1} \qquad (3)$$

with the coefficients modulating the rate of events being $a_\xi\Delta\xi = B(\gamma - 1)\alpha_\xi\Delta\xi$. This expression implies that for any given values of $S_m$ and $S_M$, the associated rate of events will have the same modulation, regardless of whether the acceptance is saturated ($\epsilon(S) = 1$) or not.

## III. Modulation of the experimental rate of events

To study the expected modulation of the rate of events, we use data taken by the SD from 1 January 2005 to 31

December 2008 with $\theta < 60°$. The events are selected on the basis of the topology and time compatibility of the triggered detectors. The station with the highest signal must be enclosed within an *active hexagon* in which all six surrounding detectors were operational at the time of the event. The value of $\rho$ at ground is deduced from P and T measured at the meteorological stations located at the central part of the array and at each FD site. Rather than using the raw number of triggering events, we compute the rate every hour normalized to the sensitive area, which is taken as the sum of the total area covered by the active hexagons every second. The modulation of the rate during the year, and as a function of the hour of the day, follows the changes in $\rho$ and P as shown in Fig. 1. Assuming that the rates of events computed each hour follow a Poisson distribution, a maximum likelihood fit gives the estimated values of the coefficients in eq. (3) averaged over the event distribution in the $\theta$ range $[0°, 60°]$:

$$\begin{aligned} a_P &= (-0.0030 \pm 0.0003)\ \mathrm{hPa}^{-1} \\ a_\rho &= (-1.93 \pm 0.04)\ \mathrm{kg}^{-1}\,\mathrm{m}^3 \\ b_\rho &= (-0.55 \pm 0.04)\ \mathrm{kg}^{-1}\,\mathrm{m}^3 \end{aligned}$$

corresponding to a reduced $\chi^2$ of 1.08. The result of the fit reproduces very well the daily averaged and the shorter term modulations of the measured rate of events as shown in Fig. 1.

## IV. Comparison among model, data and simulations

To complete the study of atmospheric effects, we performed full EAS simulations in different realistic atmospheric conditions. Proton-initiated EAS have been simulated at four fixed energies ($\log(E/\mathrm{eV}) = [18, 18.5, 19, 19.5]$), at seven fixed $\theta \in [0°, 60°]$ and for five atmospheric profiles (see Fig. 2), which are a parametrisation of the seasonal averages of several radio soundings carried out at the detector site [5]. The set of simulations consists of 60 EAS for each combination of atmospheric profile, energy and $\theta$.

The comparison of the atmospheric coefficients obtained from data with those expected from the model and simulations is shown in Fig. 3. Since we are using seasonal atmospheric profiles, we do not have access to the diurnal variation of T with the EAS simulations and thus we cannot determine the $\beta_\rho$ coefficient. In the case of the data, the dependence on $\theta$ is obtained by dividing

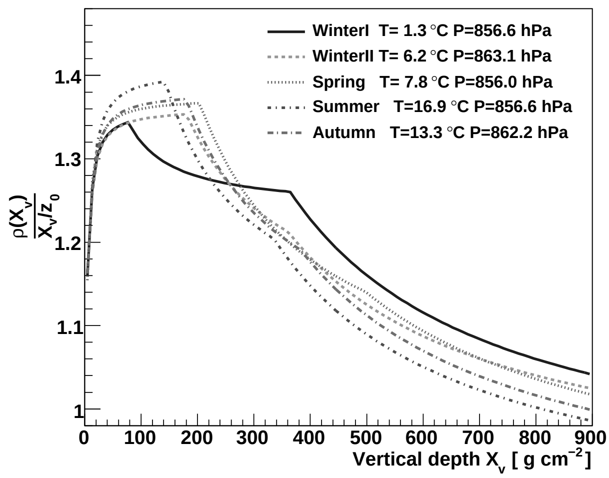


Fig. 2. Atmospheric $\rho$ profiles used in the EAS simulations normalized to an isothermal one ($X_0 = 900$ g cm$^{-2}$). These seasonal profiles come from balloon-borne sensors launched at regular intervals above the Pierre Auger Observatory site. The corresponding values of P and T are given in the box.

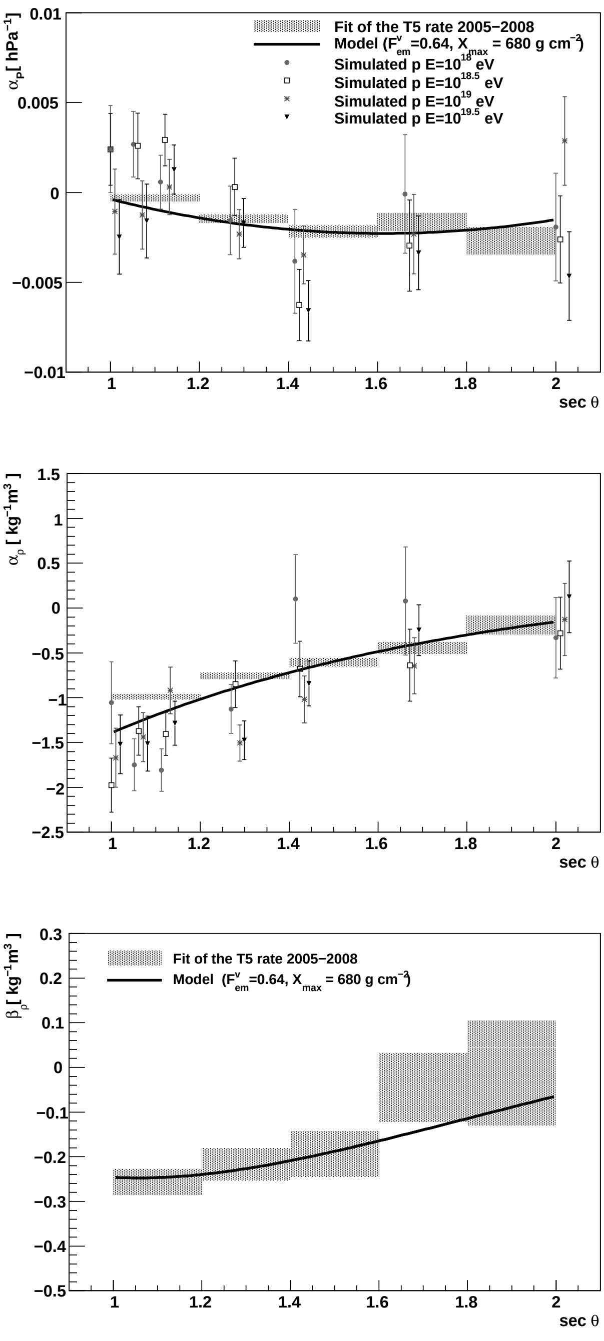


Fig. 3. Comparison of the $\alpha_P$ (top), $\alpha_\rho$ (middle) and the $\beta_\rho$ (bottom) coefficients as a function of $\sec\theta$ obtained from data (grey shaded rectangle), simulations (bullets) and model (continuous line).

the data set in subsets of equal width in $\sec\theta$. For each subset the same fitting procedure as presented previously is used. The signal coefficients are then derived dividing the rate coefficients by $B(\gamma-1)$. Since the bulk of the triggering events have $E < 10^{18}$ eV, we used the spectral index $\gamma = 3.26\pm0.04$ as measured with the Pierre Auger Observatory below $10^{18.65}$ eV [6].

## V. Correction for atmospheric effects

As explained in section II, the observed modulation in the rate of events (see Fig. 1) is due to the fact that the observed S(1000), which is used to estimate the primary energy, depends on P and $\rho$. Therefore, by applying to each event a correction of the signal, and thus of the energy, accordingly to the studied atmospheric effects, we expect to be able to obtain a non-modulated rate of events. Starting from the definition of the rate of events per unit time in a given $\theta$ bin and above a given corrected energy:

$$R(E > E_t) = \int_{E_t}^{\infty} \mathrm{d}E\, A(E)\, \frac{\mathrm{d}J}{\mathrm{d}E}$$

the relative change in the rate of events above a given energy under changes in the atmosphere is:

$$\begin{aligned}\frac{1}{R}\frac{\mathrm{d}}{\mathrm{d}\xi} R(E > E_t) &= \frac{1}{R}\int_{E_t}^{\infty} \mathrm{d}E\, \frac{\mathrm{d}A}{\mathrm{d}\xi}\, \frac{\mathrm{d}J}{\mathrm{d}E} \\ &= \frac{\alpha_\xi}{R}\int_{E_t}^{\infty} \mathrm{d}E\, \frac{\mathrm{d}\epsilon}{\mathrm{d}E}\, E\, \frac{\mathrm{d}J}{\mathrm{d}E}\end{aligned}$$

where we took for simplicity $E \propto S$. Integrating by parts, we obtain:

$$\frac{\mathrm{d}R(E > E_t)}{R\,\mathrm{d}\xi} \simeq (\gamma-1)\alpha_\xi \left(1 - \frac{\epsilon(E_t)\int_{E_t}^{\infty}\mathrm{d}E\, E^{-\gamma}}{\int_{E_t}^{\infty}\mathrm{d}E\, \epsilon(E)\, E^{-\gamma}}\right)$$

We can see that, once the energy correction is implemented, no modulation in $R(E > E_t)$ is expected above the acceptance saturation[1] since $\epsilon(E) = 1$. But, in the regime where the acceptance is not saturated the acceptance of the SD for a given corrected energy will depend on P and $\rho$. This is due to the fact that when $\epsilon(E) < 1$, the energy correction is not enough anymore to correct the rate, since, depending on atmospheric conditions, the array will trigger or not: events that do not trigger the array cannot obviously be recovered.

We have implemented the energy correction on the data set described in section III. It is done on an event-by-event basis following eq. (2). The rate of events can then be computed every hour above any given corrected energy threshold. In particular, we show in Fig. 4 the rate of events during the years and as a function of the hour of the day for corrected energies greater than $10^{18}$ eV. Even if the acceptance is not saturated at $10^{18}$ eV, the trigger efficiency is still high enough and the energy correction accounts for most of the atmospheric induced systematics. Assuming Poisson fluctuations in each bin, a fit to a constant gives a reduced $\chi^2$ of 1.30 and 1.18 for respectively the seasonal and the daily rate of events that are shown in Fig. 4.

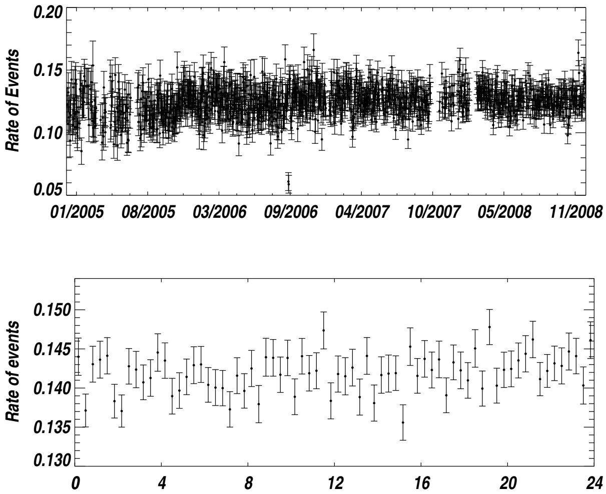


Fig. 4. Rate of events obtained above $10^{18}$ eV once the P and $\rho$ dependent conversion from signal to energy is implemented. Left: daily averaged rate of events. Right: rate of events during the day (UTC).

## VI. Conclusion

We have studied the effect of atmospheric variations on EAS measured by the array of surface detectors of the Pierre Auger Observatory. We observe a significant modulation of the rate of events with the atmospheric variables, both on seasonal scale (10%) and on a shorter time scale (2% during the day). This modulation can be explained as due to the impact of P and $\rho$ changes on the EAS development, which affect the energy estimator S(1000). Comparing the coefficients obtained from data, EAS simulations and expectations from the model built, a good agreement is reached, not only for the overall size of the effect but also for the $\theta$ dependence. By taking into account the atmospheric effects on the signal and energy estimation on a event-by-event basis, we are able to correct the observed rate of events for the seasonal modulation, thus allowing the search for large scale anisotropies at the percent level down to energies around $10^{18}$ eV [7].

## References

[1] D. Newton, *Astroparticle Physics*, **26**, (2007), 414.
[2] K. Greisen, *Progress in Cosmic Ray Physics III*, J. G. Wilson (Interscience, New York), (1956), 3.
[3] J. Abraham (Pierre Auger Collaboration), *Physical Review Letters*, **101**, (2008), 061101.
[4] M. Unger for the Pierre Auger Collaboration, *Proceedings of the 30th ICRC, Merida, Mexico*, **4**, (2007), 373.
[5] B. Keilhauer *et al.* , *Astroparticle Physics*, **22**, (2004), 249.
[6] F. Schüssler for the Pierre Auger Collaboration, *Proceedings of the 31th ICRC, Łódź, Poland*, (2009)
[7] R. Bonino for the Pierre Auger Collaboration, *Proceedings of the 31th ICRC, Łódź, Poland*, (2009)

[1] The SD trigger condition, based on a 3-station coincidence, makes the array fully efficient above about $3 \times 10^{18}$ eV.